One-Dimensional Quasiperiodic Mosaic Lattice with Exact Mobility Edges

Yucheng Wang,[1,2,3,*] Xu Xia,[4,*] Long Zhang,[2,3] Hepeng Yao,[5] Shu Chen,[6,7,8] Jiangong You,[4,†]
Qi Zhou,[4,‡] and Xiong-Jun Liu[2,3,9,1,§]

[1]*Shenzhen Institute for Quantum Science and Engineering, and Department of Physics, Southern University of Science and Technology, Shenzhen 518055, China*
[2]*International Center for Quantum Materials, School of Physics, Peking University, Beijing 100871, China*
[3]*Collaborative Innovation Center of Quantum Matter, Beijing 100871, China*
[4]*Chern Institute of Mathematics and LPMC, Nankai University, Tianjin 300071, China*
[5]*CPHT, CNRS, Institut Polytechnique de Paris, Route de Saclay 91128 Palaiseau, France*
[6]*Beijing National Laboratory for Condensed Matter Physics, Institute of Physics, Chinese Academy of Sciences, Beijing 100190, China*
[7]*School of Physical Sciences, University of Chinese Academy of Sciences, Beijing 100049, China*
[8]*Yangtze River Delta Physics Research Center, Liyang, Jiangsu 213300, China*
[9]*CAS Center for Excellence in Topological Quantum Computation, University of Chinese Academy of Sciences, Beijing 100190, China*

(Received 1 May 2020; revised 30 August 2020; accepted 15 October 2020; published 6 November 2020)

The mobility edges (MEs) in energy that separate extended and localized states are a central concept in understanding the localization physics. In one-dimensional (1D) quasiperiodic systems, while MEs may exist for certain cases, the analytic results that allow for an exact understanding are rare. Here we uncover a class of exactly solvable 1D models with MEs in the spectra, where quasiperiodic on-site potentials are inlaid in the lattice with equally spaced sites. The analytical solutions provide the exact results not only for the MEs, but also for the localization and extended features of all states in the spectra, as derived through computing the Lyapunov exponents from Avila's global theory and also numerically verified by calculating the fractal dimension. We further propose a novel scheme with experimental feasibility to realize our model based on an optical Raman lattice, which paves the way for experimental exploration of the predicted exact ME physics.

DOI: 10.1103/PhysRevLett.125.196604

Introduction.—Anderson localization (AL) is a fundamental and extensively studied quantum phenomenon, in which the disorder induces exponentially localized electronic wave functions and results in the absence of diffusion [1]. For the one and two dimensions, the states in the disordered systems are all localized [2]. For a three-dimensional (3D) system, beyond the critical disorder strength, a mobility edge (ME), which marks a critical energy E_c separating extended states from localized ones, may be resulted and can lead to novel fundamental physics [3]. For instance, varying the disorder strength or particle number density may shift the position of ME across Fermi energy and induce the metal-insulator transition. Moreover, in a system with ME only the particles of a finite energy window can flow. This can enable a strong thermoelectric response [4–6], which is widely used in thermoelectric devices. Nevertheless, it is hard to introduce microscopic models to understand the physics of the ME in 3D systems [7], so it is highly important to develop lower-dimensional models with MEs, especially with exact MEs, which allows for analytical studies.

When the random disorder is replaced by quasiperiodic potential, the system may host localized and delocalized states even in the low-dimension regime. In particular, the extended-AL transitions and MEs have been predicted in 1D quasiperiodic systems [8–19]. The simplest nontrivial example with 1D quasiperiodic potential is the Aubry-André-Harper (AAH) model [20], which shows a phase transition from a completely extended phase to a completely localized phase with increasing the strength of the quasiperiodic potential. The AAH model exhibits a self duality at the transition point for the transformation between lattice and momentum spaces. Thus no ME exists for the standard AAH model. However, by introducing a long-range hopping term [12,21,22], or breaking the self duality of the AAH Hamiltonian, e.g., superposing another quasiperiodic optical lattice [14,15,23] or introducing the spin-orbit coupling [24,25], one can obtain MEs in the energy spectra of the system. In very few cases [12,16] the self duality may be recovered on certain analytically determined energy, across which the extended-localization transition occurs, rendering the ME in the spectra, while the whole model is not exactly solvable. That is, the extended and localized states in the spectra cannot be analytically obtained to rigorously illustrate how the transition between them occurs. In consequence, to introduce and develop more generic models with MEs, which can be exactly solved beyond the dual transformation, is highly significant to further explore the rich ME physics. Moreover, it is not clear if a single system can have multiple MEs and it is important to know what determines the number of the MEs. Addressing these issues with exactly solvable models is critical to gain exact understanding of the extended-localization transition and to advance the in-depth studies of fundamental ME physics, e.g., to possibly eliminate the theoretical dispute that whether the many-body MEs exist [26,27].

The quasiperiodic systems can be easily realized in experiments in ultracold atomic gases trapped by two optical lattices with incommensurate wavelengths [28]. This configuration forms the basis of observing the AL, many-body localization, Bose glass [28–35], and, very recently, the MEs [36–39]. Experimental realization of MEs with analytic functional form can help in understanding the ME physics quantitatively and better investigate the effect of novel interacting effects on the MEs [39].

In this Letter, we propose a class of analytically solvable 1D models in quasiperiodic mosaic lattice, which hosts multiple MEs with the self-duality breaking. These models are beyond the conventional ones in which only the MEs, but not all the states of the spectra, can be precisely determined with dual transformation and can be exactly solved by applying Avila's profound global theory [40], one of his Fields Medal work, to condensed matter physics. This theory, beyond the dual transformation, gives an efficient way to calculate the Lyapunov exponent (LE) of all states. We then obtain analytically not only the exact MEs, which can be multiple here, but also the localization and extended features of all the states in the spectra. We further propose a novel scheme with experimental feasibility to realize and detect the exact MEs based on ultracold atoms.

Model.—We consider a class of quasiperiodic mosaic models, which can be described by

$$H = t\sum_j (c_j^\dagger c_{j+1} + \text{H.c.}) + 2\sum_j \lambda_j n_j, \tag{1}$$

$$\lambda_j = \begin{cases} \lambda\cos[2\pi(\omega j + \theta)], & j = m\kappa, \\ 0, & \text{otherwise}, \end{cases} \tag{2}$$

where c_j is the annihilation operator at site j, and $n_j = c_j^\dagger c_j$ is the local number operator. t, λ, and θ denote the nearest-neighbor hopping coefficient, quasiperiodic potential amplitude, and phase offset, respectively. ω is an irrational number, and κ is an integer. We set the hopping strength $t = 1$ for convenience. Since the quasiperiodic potential periodically occurs with interval κ, we can introduce a quasicell with the nearest κ lattice sites. If the quasicell number is taken as N, i.e., $m = 1, 2, \ldots, N$, the system size will be $L = \kappa N$. The quasiperiodic mosaic model with $\kappa = 2$ and $\kappa = 3$ is pictorially shown in Fig. 1, and other cases are similar.

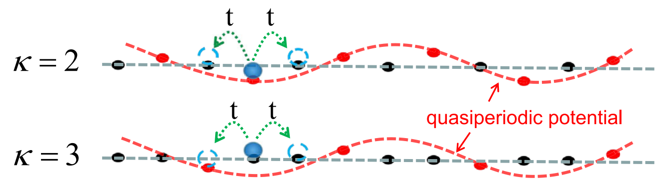

FIG. 1. The 1D quasiperiodic mosaic model with $\kappa = 2$ and $\kappa = 3$. The red and black spheres denote the lattice sites whose potentials are quasiperiodic and zero, respectively, as shown by the corresponding red and black dashed lines. The blue sphere denotes a particle, and the nearest-neighbor hopping strength is t.

It is obvious that this model reduces to the Aubry-André-Harper model when $\kappa = 1$. If $\kappa \neq 1$, the duality symmetry of these models is broken, which motivates us to show the existence of MEs. In this Letter, we prove that these models with $\kappa \neq 1$ do have energy-dependent MEs, which are given by the following expression:

$$|\lambda a_\kappa| = 1, \quad \text{for } E = E_c, \tag{3}$$

with

$$a_\kappa = \frac{1}{\sqrt{E^2-4}}\left[\left(\frac{E+\sqrt{E^2-4}}{2}\right)^\kappa - \left(\frac{E-\sqrt{E^2-4}}{2}\right)^\kappa\right]. \tag{4}$$

In addition, all the localized and extended states can be exactly studied. This is our central result, which we prove by computing the LE exactly. Before showing the analytic derivatives, we display the numerical evidence for the $\kappa = 2$ and $\kappa = 3$ cases, which benefit a visual understanding of this condition [Eq. (3)] representing it as a ME. Without loss of generality, we set $\theta = 0$ and $\omega = [(\sqrt{5}-1)/2]$, which can be approached by using the Fibonacci numbers F_n [41–43]: $\omega = \lim_{n\to\infty}(F_{n-1}/F_n)$, where F_n is defined recursively by $F_{n+1} = F_{n-1} + F_n$, with $F_0 = F_1 = 1$. We take the system size $L = F_n$ and the rational approximation $\omega = F_{n-1}/F_n$ to ensure a periodic boundary condition when numerically diagonalizing the tight-binding model defined in Eq. (1).

The $\kappa = 2$ and $\kappa = 3$ cases.—For the minimal nontrivial case with $\kappa = 2$, the two MEs read [44]

$$E_c = \pm\frac{1}{\lambda}. \tag{5}$$

For the $\kappa = 3$ case, the four MEs are given by $E_c = \pm\sqrt{1 \pm 1/\lambda}$. The numerical results are obtained from the inverse participation ratio (IPR) $\text{IPR}(m) = \sum_{j=1}^{L} |\psi_{m,j}|^4$ [3], where ψ_m is the mth eigenstate. To characterize the ME, we investigate the fractal dimension of the wave function, which is given by $\Gamma = -\lim_{L\to\infty}[\ln(\text{IPR})/\ln L]$. It is known that $\Gamma \to 1$ for extended states and $\Gamma \to 0$ for localized states. We plot energy eigenvalues and the fractal dimension Γ of the corresponding eigenstates as a function

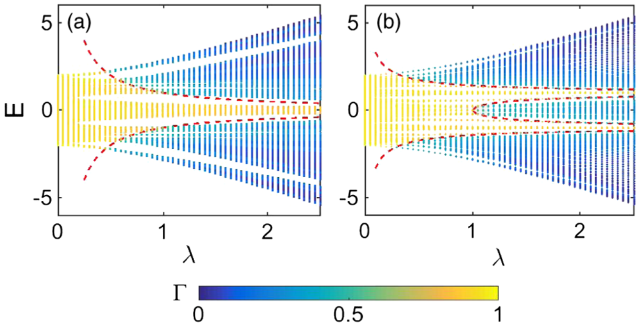

FIG. 2. Fractal dimension Γ of different eigenstates as a function of the corresponding eigenvalues and quasiperiodic potential strength λ for (a) $\kappa = 2$ with size $L = F_{14} = 610$ and (b) $\kappa = 3$ with size $L = F_{15} = 987$. The red dashed lines represent the MEs given in Eq. (3).

of potential strength λ in Fig. 2. The dashed lines in the figure represent the MEs for $\kappa = 2$ and $\kappa = 3$, respectively. As expected from the analytical results, Γ approximately changes from zero to one when the energies across the dashed lines. Further, for any κ, one can obtain $2(\kappa - 1)$ MEs well described by Eqs. (3) and (4).

The localization starts from the edges of the spectrum, as the coupling constant λ is increased, then we have MEs, and for $\kappa = 2$ MEs moves toward the center of the spectrum. This behavior is similar to MEs in the 3D disordered systems. However, the present model has a new fundamental feature that, in the arbitrarily strong quasiperiodic potential regime, the MEs always take place; i.e., the extended states always exist. This is in sharp contrast to models with random disorder and to other quasiperiodic models, where all the states are localized when the disorder is large enough. In addition, we see that the critical strength of quasiperiodic potential in extended-localization transition of the ground state is smaller than that in the standard AAH model. This is because for the mosaic lattice the particle tends to stay at the site with the smallest potential and the potential difference strongly impedes the nearest-neighbor hopping.

The ME can be further confirmed by the spatial distributions of the wave functions, as shown in Figs. 3(a) and 3(b). The wave functions for $\kappa = 2$ are localized and extended when their eigenvalues satisfy $|E| > (1/\lambda)$ and $|E| < (1/\lambda)$, respectively. It is interesting that two localization peaks are typically obtained for the localized states [see, e.g., Fig. 3(a)]. This is due to the existence of twofold degeneracy of energy levels [45], which are spatially separated from each other, as shown in Figs. 3(c) and 3(d). We have verified that most of the energy levels are twofold degenerate for any κ greater than 1. This phenomenon is related to the parent twofold degeneracy for the k and $-k$ states in the lattice model when there is no quasiperiodic potential. The interesting thing is that, while the presence of the inlaid quasiperiodic potential breaks the lattice translational symmetry and the quasimomentum is no longer a good quantum number, the twofold degeneracy is inherited in the most of the localized states.

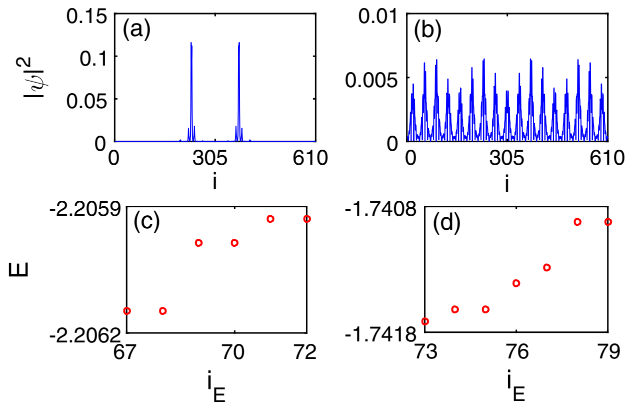

FIG. 3. Spatial distributions of two eigenstates correspond to (a) $E = -2.205(9)$ and (b) $E = -1.741(7)$, which, respectively, correspond to the nearest-neighbor eigenvalue below and above the ME of the system. Eigenenergies versus the corresponding index (c) from 67 to 72 and (d) from 73 to 79, which are, respectively, below and above the ME ($E_c = -2$), here the eigenenergies in ascending order. Here we fix $\kappa = 2$, $\lambda = 0.5$, and $L = 610$.

Rigorous mathematical proof.—Now we provide the analytical derivation for the MEs by computing the LE. Denote by $T_n(\theta)$ the transfer matrix of the Schrödinger operator [40], then LE can be computed as

$$\gamma_\epsilon(E) = \lim_{n\to\infty} \frac{1}{n} \int \ln \|T_n(\theta + i\epsilon)\| d\theta,$$

where $\|A\|$ denotes the norm of the matrix A. The complexification of the phase is important for us, since our computation relies on Avila's global theory of one-frequency analytical $SL(2,\mathbb{R})$ cocycle [40]. First note that the transfer matrix can be written as

$$T_\kappa(\theta) = \begin{pmatrix} E - 2\lambda\cos 2\pi(\theta + \kappa\omega) & -1 \\ 1 & 0 \end{pmatrix} \begin{pmatrix} E & -1 \\ 1 & 0 \end{pmatrix}^{\kappa-1},$$

where

$$\begin{pmatrix} E & -1 \\ 1 & 0 \end{pmatrix}^{\kappa-1} = \begin{pmatrix} a_\kappa & -a_{\kappa-1} \\ a_{\kappa-1} & -a_{\kappa-2} \end{pmatrix},$$

and a_κ is defined in (4). Let us then complexify the phase, and let ϵ go to infinity, then direct computation yields

$$T_\kappa(\theta + i\epsilon) = e^{2\pi\epsilon} e^{i2\pi(\theta+\kappa\omega)} \begin{pmatrix} -\lambda a_\kappa & \lambda a_{\kappa-1} \\ 0 & 0 \end{pmatrix} + o(1).$$

Thus we have $\kappa\gamma_\epsilon(E) = 2\pi\epsilon + \log|\lambda a_\kappa| + o(1)$. Avila's global theory [40,46] shows that, as a function of ϵ, $\kappa\gamma_\epsilon(E)$ is a convex, piecewise linear function, and their slopes are integers multiply 2π. This implies that $\kappa\gamma_\epsilon(E) = \max\{\ln|\lambda a_\kappa| + 2\pi\epsilon, \kappa\gamma_0(E)\}$. Moreover, by Avila's global theory, if the energy does not belong to the spectrum, if and only if $\gamma_0(E) > 0$, and $\gamma_\epsilon(E)$ is an affine function in a neighborhood of $\epsilon = 0$. Consequently, if the energy E lies in the spectrum, we have $\kappa\gamma_0(E) = \max\{\ln|\lambda a_\kappa|, 0\}$. When $|\lambda a_\kappa| > 1$, $\gamma_0(E) = (\ln|\lambda a_\kappa|/\kappa)$, the state with the energy E is localized has the localization length

$$\xi(E) = \frac{1}{\gamma_0} = \frac{\kappa}{\ln|\lambda a_\kappa|}, \tag{6}$$

which is also verified by numerical results [46]. When $|\lambda a_\kappa| < 1$, the localization length $\xi \to \infty$, and the corresponding state is delocalized. Thus, the MEs are determined by $|\lambda a_\kappa| = 1$ [i.e., Eq. (3)]. In fact, we can further show that the operator has a purely absolute continuous energy spectrum (extended states) for $|\lambda a_\kappa| < 1$, while it has a pure point spectrum for $|\lambda a_\kappa| > 1$ (localized states) [50]. This proof also shows the analytic results for the extended and localization features of all the states.

Experimental realization.—We propose the scheme of realization based on ultracold atoms. We show that the realization of the quasiperiodic mosaic model with $\kappa = 2$ is precisely mapped to the realization of a 1D lattice model with spin-1/2 atoms, whose Hamiltonian reads

$$H = \frac{k_x^2}{2m} \otimes \mathbb{1} + \mathcal{V}_p(x)\sigma_z + M_0\sigma_x + \mathcal{V}_s(x)|\downarrow\rangle\langle\downarrow|,$$
$$\mathcal{V}_p = \frac{V_p}{2}\cos(2k_p x + \phi_p), \qquad \mathcal{V}_s = \frac{V_s}{2}\cos(2k_s x + \phi_s), \tag{7}$$

where $\sigma_{x,y,z}$ are Pauli matrices, $\mathcal{V}_p(x)$ is a deep spin-dependent primary lattice with spin-conserved hopping being negligible, M_0-term couples spin-up and spin-down states, and $\mathcal{V}_s(x)$ is a secondary incommensurate potential only for spin-down atoms. One finds that the tight-binding model of H renders the quasiperiodic mosaic model with $\kappa = 2$ by mapping the spin-up (spin-down) lattice sites of the former to the odd (even) sites of the latter, the spin-flip coupling M_0-term to the hopping t-term, and the potential $\mathcal{V}_s(x)$ to the incommensurate one applied only on odd sites. This basic idea can, in principle, be generalized to realize quasiperiodic mosaic models of larger κ with higher spin systems.

The above Hamiltonian can be realized for ultracold atoms based on optical Raman lattice [see Fig. 4(a)] [51–53], as briefed below, and the details for the realization are in the Supplemental Material [46]. To facilitate the description, we transform the Hamiltonian H with the spin rotation $\sigma_x \to \sigma_z$ and $\sigma_z \to -\sigma_x$. The primary lattice then reads $-\mathcal{V}_p(x)\sigma_x$, which induces spin-flip transition in the

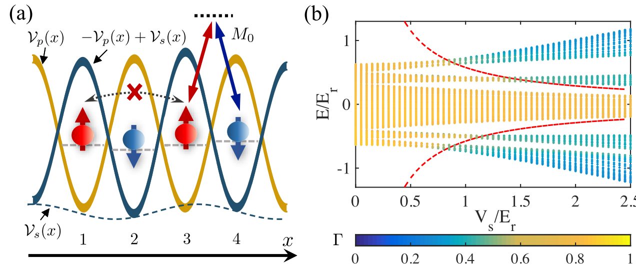

FIG. 4. Realization of the quasiperiodic model with $\kappa = 2$ in cold atoms. (a) Realization scheme. The spin-dependent primary lattice $\mathcal{V}_p(x)$ $[-\mathcal{V}_p(x)]$ locates spin-up (-down) atoms at odd (even) sites, with an incommensurate potential $\mathcal{V}_s(x)$ being applied only to the spin-down atoms. The primary lattice is deep enough such that the spin-conserved hopping can be ignored. A Raman coupling M_0 is then used to induce the spin-flipped hopping, which plays the role of nearest-neighbor tunneling. (b) Fractal dimension Γ of the lowest-band eigenstates of the lattice model as a function of the lattice depth V_s. The eigenvalues E have been shifted a constant value such that the center of the band is zero for $V_s = 0$. Here we set $V_p = 10E_r$, $M_0 = 1.5E_r$, and $k_s/k_p = [(\sqrt{5}-1)/2]$, with $E_r \equiv k_p^2/(2m)$. The red dashed curves represent the analytical MEs $E_c = \pm t^2/\lambda$, with $t \simeq 0.353E_r$ and $\lambda \simeq 0.215V_s$.

new bases and can be generated by a two-photon Raman process driven by two laser beams $\mathbf{E}_{1,2}$ in the form $\propto \mathbf{E}_1^*\mathbf{E}_2 \sim \cos(2k_p x)$ (see Supplemental Material [46]). The incommensurate lattice can be similarly obtained by a combination of two potentials $(\mathcal{V}_s/2)\sigma_x$ and $-(\mathcal{V}_s/2)\mathbb{1}$ with $\mathcal{V}_s(x) = (V_s/2)\sin(2k_s x)$, of which the former is a two-photon Raman coupling potential induced by another two standing-wave beams $\mathbf{E}_{3,4}$ in the form $\propto \mathbf{E}_3^*\mathbf{E}_4$, with $(\mathbf{E}_3, \mathbf{E}_4) \sim (\cos(k_s x), \sin(k_s x))$, while the latter is a standard spin-independent lattice. Finally, the M_0-term is directly given by the two-photon detuning (δ) of the Raman coupling processes, taking the form $(\delta/2)\sigma_z$. After performing the inverse spin-rotation transformation on these terms, we reach the Hamiltonian (7). More details can be found in the Supplemental Material [46], where ^{40}K atoms are employed to illustrate the realization.

Finally, we estimate the parameter regimes for the realization. In experiment, one should set a large V_p compared with (M_0, V_s), such that the spin-conserved hopping t_p (mimicking the next-nearest-neighbor hopping) is negligible. For example, when $V_p = 10E_r$ and $M_0 = 1.5E_r$ with $E_r \equiv k_p^2/(2m)$, we have $t \simeq 18.3t_p$ [46]. Thus, regardless of the atom spin and taking into account only s bands, this lattice Hamiltonian (7) indeed leads to the tight-binding model described by Eq. (1) with $\kappa = 2$. To further verify our realization scheme, we calculate the fractal dimension Γ of the lowest-band eigenstates of the Hamiltonian (7) and show the results as a function of the lattice depth V_s in Fig. 4(b). It can be seen that the distributions of localized and extended states are very similar to the results in Fig. 2(a). We then check the analytical expressions for MEs: $E_c = \pm t^2/\lambda$, where the nearest-neighbor tunneling t and the quasiperiodic potential strength $\lambda \propto V_s$ can be derived based on s-band Wannier functions in the tight-binding limit [46]. We plot the results as red dashed curves in Fig. 4(b) and find them in good agreement with the fractal dimension calculations. In experiment, one can determine the MEs by observing the time evolution of an initial charge-density wave state [36], detecting the interference pattern [29] or characterizing the correlation length [33,54].

Conclusion.—We have proposed a class of exactly solvable 1D mosaic models to realize MEs in energy spectra, where quasiperiodic on-site potentials are inlaid in the lattice with equally spaced sites, and proposed the experimental realization. By calculating the Lyapunov exponents, we have analytically demonstrated the existence of MEs and obtained their expressions, which are in excellent agreement with the numerical studies. For the integer inlay parameter $\kappa > 1$ of our proposed models, one obtains $2(\kappa - 1)$ MEs, which are symmetrically distributed in energy spectra and always exist even in the strong quasiperiodic potential regime. Our work uncovers a variety of new lattice models that host multiple exact MEs and opens a new avenue to analytically explore novel ME physics with experimental feasibility.

We thank Laurent Sanchez-Palencia for helpful comments. Y. W., L. Z., and X.-J. L. are supported by National Nature Science Foundation of China (11825401, 11761161003, and 11921005), the National Key R&D Program of China (2016YFA0301604), Guangdong Innovative and Entrepreneurial Research Team Program (No. 2016ZT06D348), the Science, Technology and Innovation Commission of Shenzhen Municipality (KYTDPT20181011104202253), and the Strategic Priority Research Program of Chinese Academy of Science (Grant No. XDB28000000). S. C. was supported by the NSFC (Grant No. 11974413) and the NKRDP of China (Grants No. 2016YFA0300600 and No. 2016YFA0302104). H. Y. acknowledges the support from the Paris region DIM-SIRTEQ. X. X. is supported by the NanKai Zhide Foundation. J. Y. was partially supported by NSFC Grant No. 11871286 and the Nankai Zhide Foundation. Q. Z. was partially supported by NSFC Grants No. 11671192 and No. 11771077 and the Nankai Zhide Foundation.

*These authors contributed equally to this work.
†jyou@nankai.edu.cn
‡qizhou@nankai.edu.cn
§xiongjunliu@pku.edu.cn

[1] P. W. Anderson, Absence of diffusion in certain random lattices, Phys. Rev. **109**, 1492 (1958).

[2] E. Abrahams, P. W. Anderson, D. C. Licciardello, and T. V. Ramakrishnan, Scaling Theory of Localization: Absence of Quantum Diffusion in Two Dimensions, Phys. Rev. Lett. **42**, 673 (1979).

[3] F. Evers and A. D. Mirlin, Anderson transitions, Rev. Mod. Phys. **80**, 1355 (2008).

[4] R. Whitney, Most Efficient Quantum Thermoelectric at Finite Power Output, Phys. Rev. Lett. **112**, 130601 (2014).

[5] C. Chiaracane, M. T. Mitchison, A. Purkayastha, G. Haack, and J. Goold, Quasiperiodic quantum heat engines with a mobility edge, Phys. Rev. Research **2**, 013093 (2020).

[6] K. Yamamoto, A. Aharony, O. Entin-Wohlman, and N. Hatano, Thermoelectricity near Anderson localization transitions, Phys. Rev. B **96**, 155201 (2017).

[7] A. Purkayastha, A. Dhar, and M. Kulkarni, Non-equilibrium phase diagram of a 1D quasiperiodic system with a single-particle mobility edge, Phys. Rev. B **96**, 180204(R) (2017).

[8] S. Das Sarma, S. He, and X. C. Xie, Mobility Edge in a Model One-Dimensional Potential, Phys. Rev. Lett. **61**, 2144 (1988).

[9] Y. Hashimoto, K. Niizeki, and Y. Okabe, A finite-size scaling analysis of the localization properties of one-dimensional quasiperiodic systems, J. Phys. A **25**, 5211 (1992).

[10] D. J. Boers, B. Goedeke, D. Hinrichs, and M. Holthaus, Mobility edges in bichromatic optical lattices, Phys. Rev. A **75**, 063404 (2007).

[11] J. Biddle, B. Wang, D. J. Priour Jr, and S. Das Sarma, Localization in one-dimensional incommensurate lattices beyond the Aubry-André model, Phys. Rev. A **80**, 021603(R) (2009).

[12] J. Biddle and S. Das Sarma, Predicted Mobility Edges in One-Dimensional Incommensurate Optical Lattices: An Exactly Solvable Model of Anderson Localization, Phys. Rev. Lett. **104**, 070601 (2010).

[13] S. Lellouch and L. Sanchez-Palencia, Localization transition in weakly-interacting Bose superfluids in one-dimensional quasiperiodic lattices, Phys. Rev. A **90**, 061602(R) (2014).

[14] X. Li, X. Li, and S. Das Sarma, Mobility edges in one dimensional bichromatic incommensurate potentials, Phys. Rev. B **96**, 085119 (2017).

[15] H. Yao, H. Khoudli, L. Bresque, and L. Sanchez-Palencia, Critical Behavior and Fractality in Shallow One-Dimensional Quasiperiodic Potentials, Phys. Rev. Lett. **123**, 070405 (2019).

[16] S. Ganeshan, J. H. Pixley, and S. Das Sarma, Nearest Neighbor Tight Binding Models with an Exact Mobility Edge in One Dimension, Phys. Rev. Lett. **114**, 146601 (2015).

[17] Z. Xu, H. Huangfu, Y. Zhang, and S. Chen, Dynamical observation of mobility edges in one-dimensional incommensurate optical lattices, New J. Phys. **22**, 013036 (2020).

[18] Y. Liu, X.-P. Jiang, J. Cao, and S. Chen, Non-Hermitian mobility edges in one-dimensional quasicrystals with parity-time symmetry, Phys. Rev. B **101**, 174205 (2020).

[19] Q.-B. Zeng and Y. Xu, Winding numbers and generalized mobility edges in non-Hermitian systems, Phys. Rev. Research **2**, 033052 (2020).

[20] S. Aubry and G. André, Analyticity breaking and Anderson localization in incommensurate lattices, Ann. Isr. Phys. Soc. **3**, 133 (1980).

[21] X. Deng, S. Ray, S. Sinha, G. V. Shlyapnikov, and L. Santos, One-Dimensional Quasicrystals with Power-Law Hopping, Phys. Rev. Lett. **123**, 025301 (2019).

[22] M. Saha, S. K. Maiti, and A. Purkayastha, Anomalous transport through algebraically localized states in one dimension, Phys. Rev. B **100**, 174201 (2019).

[23] H. Yin, J. Hu, A.-C. Ji, G. Juzeliunas, X.-J. Liu, and Q. Sun, Localization Driven Superradiant Instability, Phys. Rev. Lett. **124**, 113601 (2020).

[24] L. Zhou, H. Pu, and W. Zhang, Anderson localization of cold atomic gases with effective spin-orbit interaction in a quasiperiodic optical lattice, Phys. Rev. A **87**, 023625 (2013).

[25] M. Kohmoto and D. Tobe, Localization problem in a quasiperiodic system with spin-orbit interaction, Phys. Rev. B **77**, 134204 (2008).

[26] W. De Roeck, F. Huveneers, M. Müller, and M. Schiulaz, Absence of many-body mobility edges, Phys. Rev. B **93**, 014203 (2016).

[27] X. B. Wei, C. Cheng, G. Xianlong, and R. Mondaini, Investigating many-body mobility edges in isolated quantum systems, Phys. Rev. B **99**, 165137 (2019).

[28] G. Roati, C. D'Errico, L. Fallani, M. Fattori, C. Fort, M. Zaccanti, G. Modugno, M. Modugno, and M. Inguscio, Anderson localization of a non-interacting Bose-Einstein condensate, Nature (London) **453**, 895 (2008).

[29] L. Fallani, J. E. Lye, V. Guarrera, C. Fort, and M. Inguscio, Ultracold Atoms in a Disordered Crystal of Light: Towards a Bose Glass, Phys. Rev. Lett. **98**, 130404 (2007).

[30] M. Schreiber, S. S. Hodgman, P. Bordia, H. P. Lüschen, M. H. Fischer, R. Vosk, E. Altman, U. Schneider, and I. Bloch, Observation of many-body localization of interacting fermions in a quasirandom optical lattice, Science **349**, 842 (2015).

[31] P. Bordia, H. P. Lüschen, S. S. Hodgman, M. Schreiber, I. Bloch, and U. Schneider, Coupling Identical One-Dimensional Many-Body Localized Systems, Phys. Rev. Lett. **116**, 140401 (2016).

[32] P. Bordia, H. Lüschen, S. Scherg, S. Gopalakrishnan, M. Knap, U. Schneider, and I. Bloch, Probing Slow Relaxation and Many-Body Localization in Two-Dimensional Quasiperiodic Systems, Phys. Rev. X **7**, 041047 (2017).

[33] C. D'Errico, E. Lucioni, L. Tanzi, L. Gori, G. Roux, I. P. McCulloch, T. Giamarchi, M. Inguscio, and G. Modugno, Observation of a Disordered Bosonic Insulator from Weak to Strong Interactions, Phys. Rev. Lett. **113**, 095301 (2014).

[34] H. P. Lüschen, P. Bordia, S. Scherg, F. Alet, E. Altman, U. Schneider, and I. Bloch, Observation of Slow Dynamics near the Many-Body Localization Transition in One-Dimensional Quasiperiodic Systems, Phys. Rev. Lett. **119**, 260401 (2017).

[35] Y. Wang, X.-J. Liu, and D. Yu, Many-body critical phase: Extended and nonthermal, arXiv:1910.12080.

[36] H. P. Lüschen, S. Scherg, T. Kohlert, M. Schreiber, P. Bordia, X. Li, S. D. Sarma, and I. Bloch, Single-Particle Mobility Edge in a One-Dimensional Quasiperiodic Optical Lattice, Phys. Rev. Lett. **120**, 160404 (2018).

[37] F. A. An, E. J. Meier, and B. Gadway, Engineering a Flux-Dependent Mobility Edge in Disordered Zigzag Chains, Phys. Rev. X **8**, 031045 (2018).

[38] T. Kohlert, S. Scherg, X. Li, H. P. Lüschen, S. D. Sarma, I. Bloch, and M. Aidelsburger, Observation of Many-Body Localization in a One-Dimensional System with Single-Particle Mobility Edge, Phys. Rev. Lett. **122**, 170403 (2019).

[39] F. A. An, K. Padavić, E. J. Meier, S. Hegde, S. Ganeshan, J. H. Pixley, S. Vishveshwara, and B. Gadway, Observation of tunable mobility edges in generalized Aubry-André lattices, arXiv:2007.01393.

[40] A. Avila, Global theory of one-frequency Schrödinger operators, Acta. Math. **1**, 215 (2015).

[41] M. Kohmoto, Metal-Insulator Transition and Scaling for Incommensurate Systems, Phys. Rev. Lett. **51**, 1198 (1983).

[42] Y. Wang, Y. Wang, and S. Chen, Spectral statistics, finite-size scaling and multifractal analysis of quasiperiodic chain with p-wave pairing, Eur. Phys. J. B **89**, 254 (2016).

[43] Y. Wang, L. Zhang, S. Niu, D. Yu, and X.-J. Liu, Realization and Detection of Non-Ergodic Critical Phases in Optical Raman Lattice, Phys. Rev. Lett. **125**, 073204 (2020).

[44] We note that, in the limit $|E| = 2$, we shall find $|a_\kappa(\pm 2)| = \kappa$.

[45] Figure 3(a) plots the wave function of one of the two degenerate states. We note that by properly choosing linear combinations of the two degenerate levels, one can construct two orthogonal states with each having only one peak.

[46] See Supplemental Material at http://link.aps.org/supplemental/10.1103/PhysRevLett.125.196604 for details on (I) multifractal analysis, (II) some mathematical basis of computing the Lyapunov exponent, (III) localization length, and (IV) experimental realization. The Supplemental Material includes Refs. [25,40,47–49].

[47] H. Hiramoto and M. Kohmoto, Scaling analysis of quasiperiodic systems: Generalized Harper model, Phys. Rev. B **40**, 8225 (1989).

[48] J. Wang, X.-J. Liu, G. Xianlong, and H. Hu, Phase diagram of a non-Abelian Aubry-André-Harper model with p-wave superfluidity, Phys. Rev. B **93**, 104504 (2016).

[49] T. G. Tiecke, Properties of potassium, 2011, http://www.tobiastiecke.nl/archive/PotassiumProperties.pdf.

[50] X. Xia, J. You, Z. Zheng, and Q. Zhou (to be published).

[51] B.-Z. Wang, Y.-H. Lu, W. Sun, S. Chen, Y. Deng, and X.-J. Liu, Dirac-, Rashba-, and Weyl-type spin-orbit couplings: Toward experimental realization in ultracold atoms, Phys. Rev. A **97**, 011605(R) (2018).

[52] W. Sun, B.-Z. Wang, X.-T. Xu, C.-R. Yi, L. Zhang, Z. Wu, Y. Deng, X.-J. Liu, S. Chen, and J.-W. Pan, Highly Controllable and Robust 2D Spin-Orbit Coupling for Quantum Gases, Phys. Rev. Lett. **121**, 150401 (2018).

[53] B. Song, L. Zhang, C. He, T. F. J. Poon, E. Hajiyev, S. Zhang, X.-J. Liu, and G.-B. Jo, Observation of symmetry-protected topological band with ultracold fermions, Sci. Adv. **4**, eaao4748 (2018).

[54] H. Yao, T. Giamarchi, and L. Sanchez-Palencia, Lieb-Liniger Bosons in a Shallow Quasiperiodic Potential: Bose Glass Phase and Fractal Mott Lobes, Phys. Rev. Lett. **125**, 060401 (2020).